98% Efficient Single-Stage AC/DC Converter Topologies

A new Hybrid Switching Method is introduced in this article which for the first time makes possible AC/DC power conversion in a single power processing stage providing both Power Factor Correction and isolation at high switching frequency. This single-phase rectifier is extended to a three-phase rectifier, which for the first time enables direct conversion from three-phase input power to output DC power resulting simultaneously in the highest efficiency and lowest size. **Slobodan Ćuk, President TESLAco, Irvine, USA**

The goal of developing AC/DC converters with Isolation and Power Factor Correction (PFC) feature in a single power processing stage and without a mandatory full-bridge rectifier has for years eluded power electronics researchers (see cover image). Present AC/DC converters operated from a single-phase AC line are based on conventional Pulse Width Modulation (PWM) switching and process the power through at least three distinct power processing stages: full-bridge rectifier followed by boost PFC converter and another cascaded isolated full-bridge DC/DC converter stage, which together use a total of 14 switches and three magnetic components resulting in corresponding efficiency, size and cost limitations.

The new Hybrid Switching Method enables new Single-Stage AC/DC converter topology, the True Bridgeless PFC Converter* consisting of just three switches and a single magnetic component albeit at a much higher efficiency approaching 98%, having a 0.999 power factor and 1.7% total harmonic distortion. Three-Phase Rectifier* consisting of three such Single-Phase Rectifiers* (*US and foreign patents pending) takes for the first time a full advantage of Tesla's three-phase transmission system to convert constant instantaneous input power of a three-phase system directly to a constant DC output power, albeit isolated at high switching frequency, with near unity power factor (0.999), low total harmonic distortion (1.7%), smaller size and lower cost but at ultra high efficiency of 98% [6].

Serbian-American inventor Nikola Tesla in 1879 invented the three-phase) transmission system, which together AC three-phase motors and AC generators enabled a very efficient worldwide electric power transmission and utilization, which is still unsurpassed today. One of the key properties of Tesla's three-phase system is that it consists of three AC voltages each displaced from the other by 120 degrees. When each phase is delivering the current in phase and proportional to its respective AC line voltage (unity power factor operation on each phase), the instantaneous power from each phase is positive (active) and is time varying. Nevertheless, the sum of the powers of all three phases is constant in time (see Figure 1). As this property is available on both three-phase AC generator side and three-phase AC load side there is no electrical energy storage needed in such a three-phase long distance transmission system. Yet, availability of the AC voltages on each side, make possible use of the three phase AC transformers for stepping up the AC voltage on generator side and stepping-down AC voltage on the users load side.

New boost converter topologies

The new Hybrid Switching Method can best be explained by way of an example. Shown in Figure 2a is the Ćuk converter [1,2] modified by the insertion of the current rectifier CR_1 in series with the output inductor which is now designated as L_r where index r signifies a qualitatively changed role of that inductor: from a PWM inductor in Square-Wave switching Ćuk converter to the resonant inductor. The elimination of the PWM inductor also eliminates the inherent step-down conversion characteristic of the Ćuk converter and leaves only its step-up DC voltage gain, albeit with the polarity inversion of the Ćuk converter remaining intact. Thus, the new DC voltage gain is

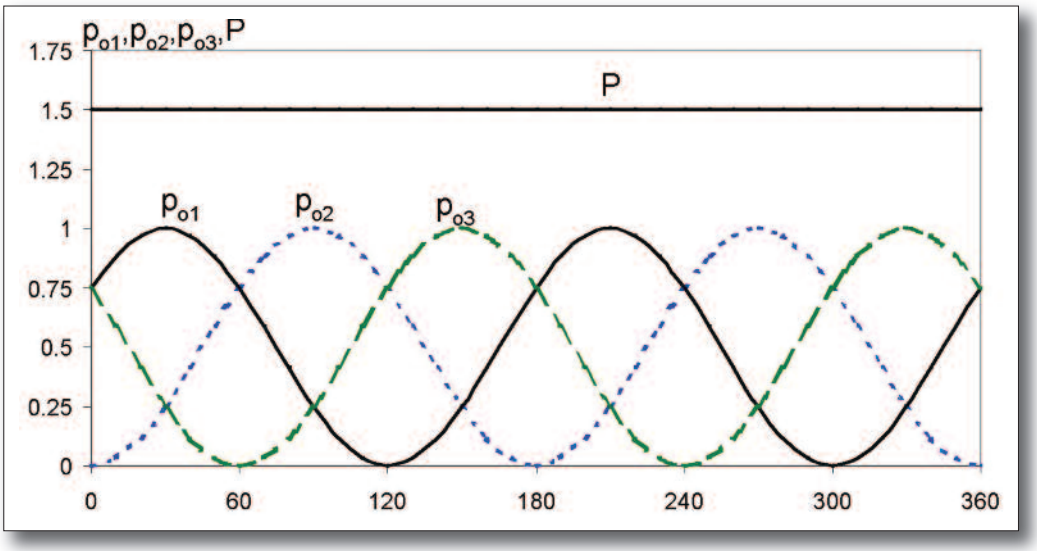

Figure 1: In Tesla's three-phase system the sum of the power of all three phases is constant in time

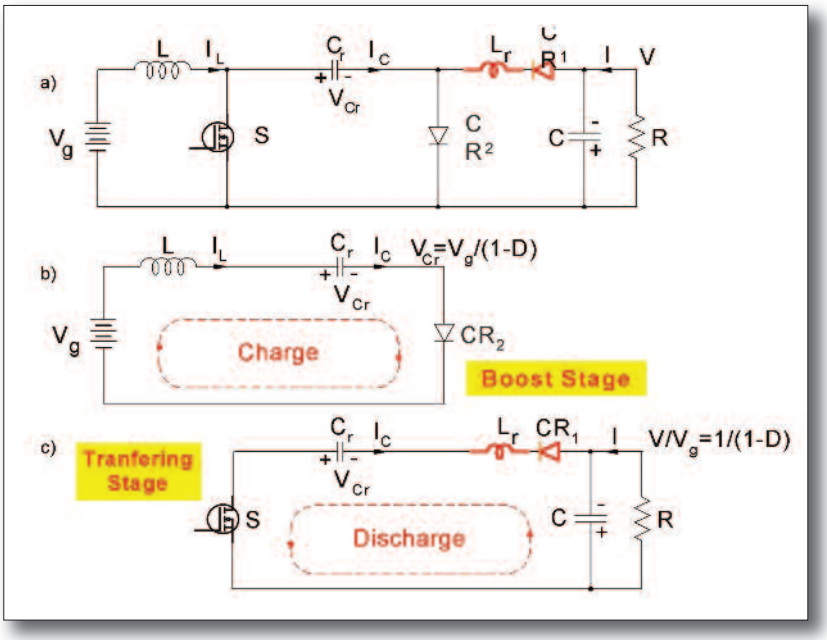

Figure 2: Hybrid Switching Method with (a) Ćuk converter modified by the insertion of the current rectifier in series with the output inductor, (b) controlling switch S for the boost stage, and at the same time also a controlling switch for the translation stage (c)

according to equation 1:

$$\frac{V}{V_g} = -\frac{1}{1-D} \qquad (1)$$

Thus, we already obtained a new polarity inverting type of the boost converter, which did not exist before. Let us now examine a more closely the operation of the polarity inverting boost converter. First, it consist of three switches, one active controlling switch S (MOSFET) and two current rectifiers CR_1 and CR_2. This is already in contrast to all existing conventional Square-wave PWM switching converters which explicitly exclude odd number of switches such as 3 in this case, as the switches must come in complementary pairs, hence 2, 4, or more but even number of switches.

Note a dual role of the controlling switch S: it is the controlling switch for the boost stage highlighted in Figure 2b but at the same time also a controlling switch for the translation stage highlighted in Figure 2c. Note also the role of the resonant capacitor C_r connecting two stages, the boost and transferring stage: as an output PWM capacitor of the boost stage charging linearly during the OFF-time interval by the input inductor current source, and as a resonant capacitor discharging resonantly during the subsequent ON-time transferring stage into the load.

Figure 3 shows the resonant circuit model and corresponding resonant capacitor waveform for entire switching period. The instantaneous resonant capacitor voltage is continuous at the switching instants (no jump in voltages at those instances) with a superimposed DC voltage level equal to V_C. As the resonance of this capacitor is clearly contained exclusively during the ON-time discharging interval DT_S the resonant circuit model imposes that flux balance on the resonant inductor must be fulfilled during this interval alone, resulting in steady-state condition according to equation 2:

$$\int v_{Cr}\,dt = V_{Cr} - V = 0 \qquad (2)$$

This now also puts a spotlight on the significance of the role of the resonant inductor. In its absence, this transfer of charge will be taking place but in a dissipative way thus resulting in much reduced efficiency and in additional spike voltages on switches. The resonant inductor L_r solves both of these problems.

From (2) the resonant capacitor voltage in Figure 3 has a DC voltage V_{Cr} superimposed on the AC ripple voltage Δv_C. As the output capacitor C is much larger then resonant capacitor C_r their series connection results in a resonant model of Figure 4, which has resonant capacitor C_r only left in the resonant model. Moreover, the net voltage on this resonant capacitor is a ripple voltage Δv_{Cr} as the DC voltages subtract as per (2). The corresponding time domain waveform of the resonant capacitor current is as in Figure 4.

From Figure 2a the capacitor resonant discharge current has a diode CR_1 in the

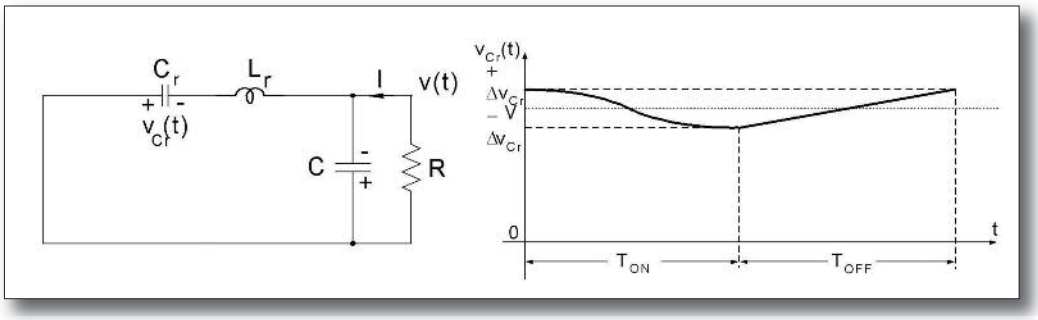

Figure 3: Resonant circuit model and corresponding resonant capacitor waveform for the entire switching period

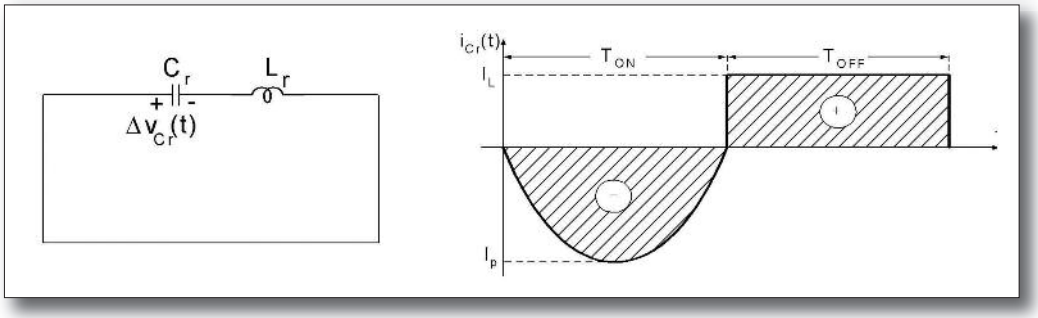

Figure 4: Corresponding time domain waveform of the resonant capacitor current

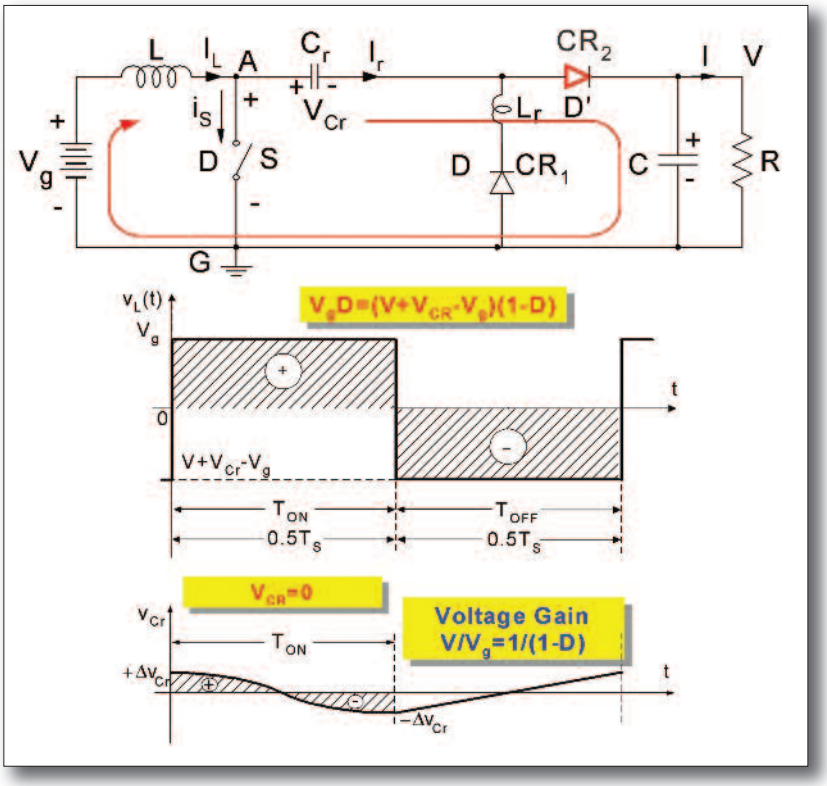

Figure 5: Companion polarity non-inverting boost converter with (a) relocated resonance inductor and (b) flux balance on resonant and PWM inductor

discharge loop. This diode permits only the positive flow of current in the direction dictated by the diode. Moreover, the diode cannot turn-OFF until the resonant inductor current is reduced to zero at the end of ON-time interval, hence resonant capacitor current is also zero as illustrated in the resonant capacitor current waveform in Figure 4. Since the resonant current is full-wave sinusoidal waveform, the resonant capacitor current also must start at zero current level at the beginning of the ON-time interval as illustrated in Figure 4 as well.

From the resonant AC circuit model in Figure 5 the solutions for resonant current and voltage are according to equations 3/4:

$$i_r(t) = I_P \sin(\omega_r t) \quad v_{Cr}(t) = \Delta v_{Cr} \cos(\omega_r t) \quad (3)$$

$$\Delta v_{Cr} = I_P R_N \quad R_N = \sqrt{L_r/C_r} \quad \omega_r = \frac{1}{2\pi\sqrt{L_r C_r}} \quad (4)$$

A companion polarity non-inverting boost converter can be easily obtained by simply inverting the polarity of the two output current rectifiers in Figure 2a and relocating L_r to result in the converter of Figure 5a. Note that current rectifiers are also changing designation since CR_2 rectifier is now conducting during OFF-time interval just as in conventional boost converter. The flux balance on resonant inductor and PWM inductor as shown in Figure 5b results according to equations 5/6 in:

$$V_{Cr} = 0 \quad (5)$$

$$V_g = \frac{1}{1-D} \quad (6)$$

Yet another converter topology is shown in Figure 6a in which the input voltage source has a negative polarity resulting in positive polarity of the output DC voltage and corresponding AC flux balance shown in shaded areas in Figure 6b. Note that this converter topology is analogous to the original polarity inverting boost topology of Figure 2a but with the source voltage being negative. Therefore the same results as previously derived are obtained for steady-state DC voltages. Note the change of the placement of the resonant inductor to the branch with the rectifier CR_2. As the resonant capacitor ripple voltage Δv_r is an order of magnitude smaller than DC voltage V_r, the flux of the resonant inductor is some 50 times smaller than that of PWM inductor as seen by comparing shaded areas of the PWM inductor and resonant inductor. Clearly this results in resonant inductor physical size and losses being negligible compared to PWM input inductor.

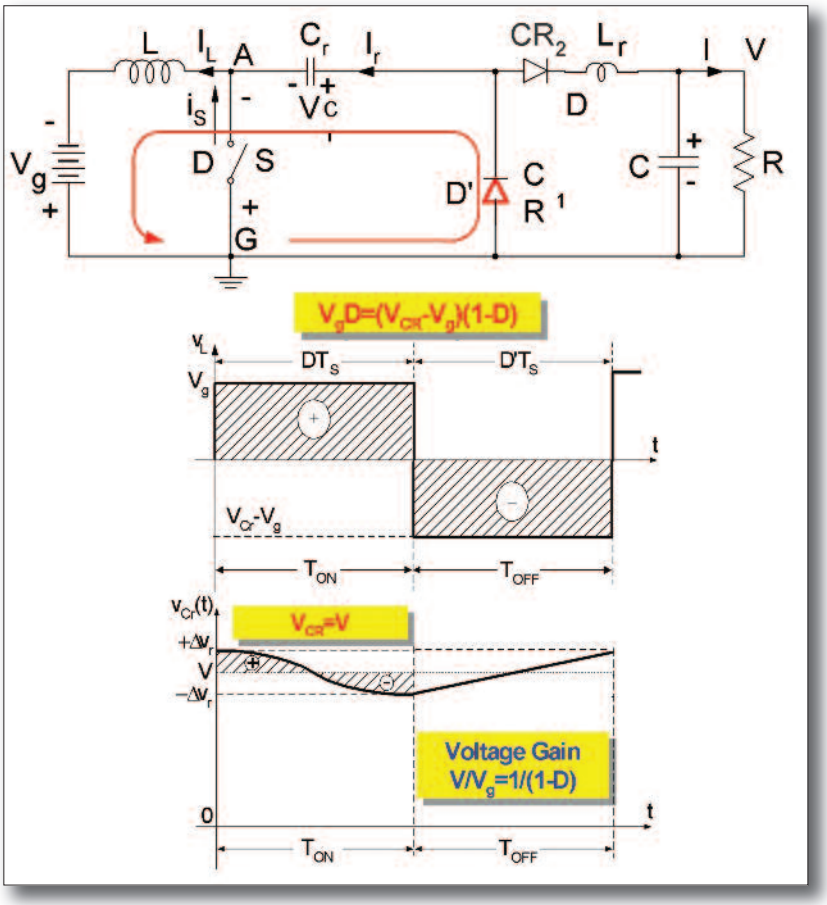

Figure 6: Inverting boost topology of Figure 3a but with the source voltage being negative (a) and AC flux balance shown in shaded areas (b)

True bridgeless PFC converter topology

Comparison of the converter topologies in Figures 2a/6a reveals that the polarity change of the input source voltage results

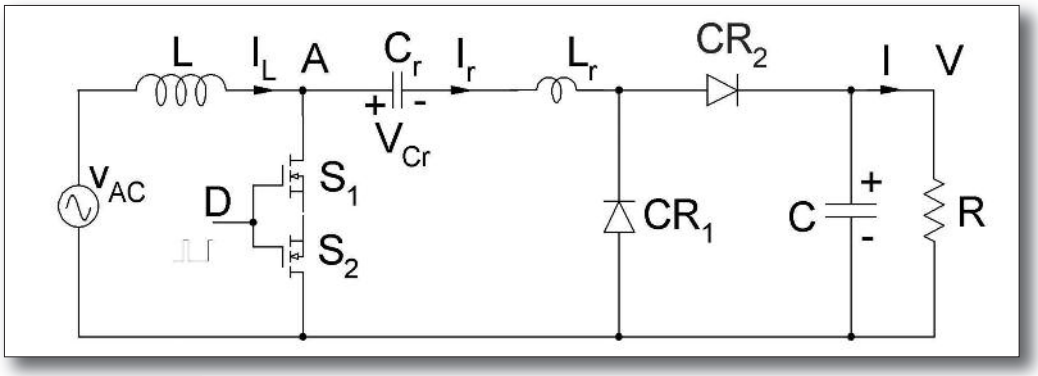

Figure 7: Topologically invariant converter which does not change its structure irrespective of the polarity of the source voltage

in positive and equal output DC voltages given by (1) and (6), respectively. However, only one obstacle remains to make these two topologies invariant relative to the polarity change of the input voltage source and that is switching of the resonant inductor L_r placement from one diode branch to another. This problem can be solved by placing resonant inductor for both cases in branch with the resonant capacitor C_r as illustrated in the converter of Figure 7. This now results in topologically invariant converter of Figure 7, which does not change its structure irrespective of the polarity of the source voltage. Therefore, the source voltage can be an AC voltage v_{AC} which changes its polarity as shown in Figure 7.

Note how the polarity of the input source automatically dictates which of the two rectifiers should be conducting during which interval. Stated alternatively, the full-bridge rectifier on the front end is not needed any more since the new converter topology operates as the first true AC/DC converter with the same DC voltage gain for either polarity of input voltage. As the result we obtained an AC/DC single-stage True Bridgeless PFC converter which can operate directly from the AC line and without front-end bridge rectifier common to conventional PFC boost converters. As the controlling switch S must change its current direction and voltage blocking capability depending on the polarity of the AC line voltage, it is implemented by a series back-to-back connection of two MOSFET switches.

In conventional boost converters there are no good ways to introduce the isolation. The most popular is the Full-Bridge Isolated Boost converter, which consists of four active controlling MOSFET switches on the primary side and four-diode bridge on the secondary side. The isolation transformer in the True Bridgeless PFC converter, however, is introduced in Figure 8 which preserves the original three-switch configuration and other advantageous of the original non-isolated configurations, such as low voltage stresses on all switches.

By controlling the input AC line current (at 50/60Hz) so that it is in phase and

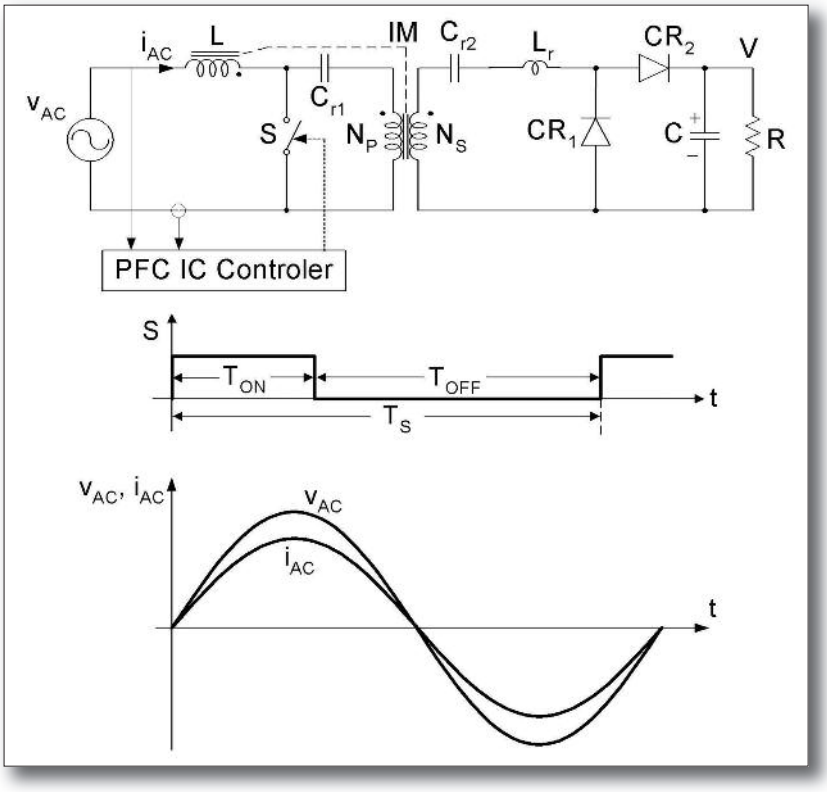

Figure 8: True Bridgeless PFC Converter with isolation

proportional to input AC line voltage (Figure 8), the unity power factor and low total harmonic distortion can be obtained. Note also that the PFC IC controller must also be a True Bridgeless PFC controller, as it needs to accept as its inputs the full-wave AC line voltage and full-wave AC line currents. Current PFC IC controllers, on the other hand have as input rectified AC line voltage and rectified AC line current. These conventional PFC IC controllers could still be used but with additional signal processing circuitry converting full-wave AC voltage and full-wave AC line current into half-rectified ac waveform for use with standard PFC IC controller.

The isolation transformer is of the best kind (single-ended transformer of the Ćuk converter type) having magnetic core with the BH loop as illustrated in Figure 9 with bi-directional flux capability and square-loop characteristic, as there is no DC-bias in the transformer operation. Therefore, the design could be scaled up to high

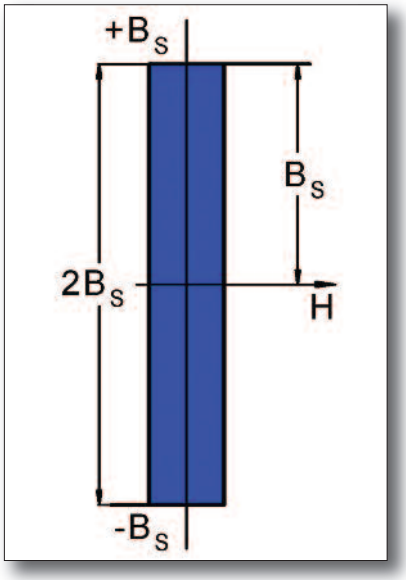

Figure 9: Isolation transformer having magnetic core with bi-directional flux capability and square-loop characteristic

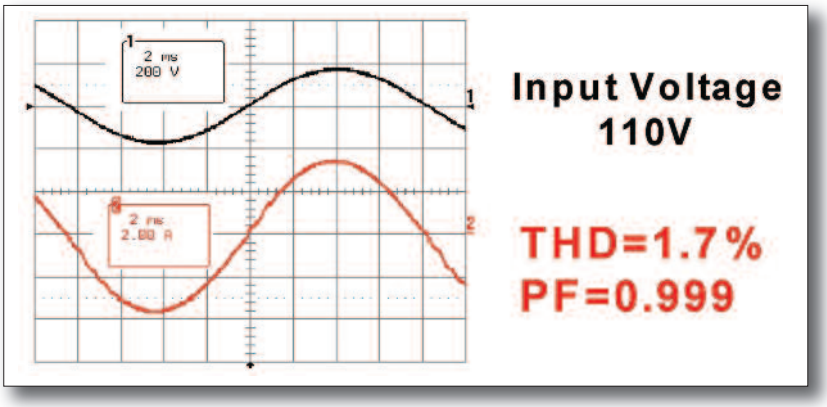

Figure 10: PFC performances measured on the prototype of a 400W, AC/DC Bridgeless PFC converter and the measurement results obtained at 300W power level

power without the degradation of the performance or the large size of magnetic core. In fact, the isolation transformer has AC flux, which is at least four times lower than the flux in, for example, forward converter and bridge-type isolated converters. This directly translates in proportionally reduced size of the magnetics and increased efficiency.

Further improvements are obtained by integration of the input inductor onto a common core with the isolation transformer [1,2,3, 5]. The placement of the air-gap on the magnetic leg with isolation transformer winding results in shifting of the input inductor high switching frequency ripple to the isolation transformer resulting in ripple-free input current as seen in Figure 8 in addition to reduction of magnetics size to one magnetic core only and further efficiency improvements.

The PFC performances is measured on the prototype of a 400W, AC/DC Bridgeless PFC converter and the measurement results obtained at a 300W power level shown in Figure 10 exhibit a low total harmonic distortion of 1.7% and a power factor of 0.999. The efficiency measurements in Figure 11 show near 98% efficiency at high line of 240V AC. Most important is that at 120V AC line (US main) efficiency is also very high (97.2%) as the usual efficiency degradation of 2% to 3% at low line due to the two-diode drops of the front-end bridge rectifiers are eliminated.

Three-Phase Bridgeless Rectifier

All present AC/DC converters are based on the cascade of at least two power processing stages. The first stage converts the three-phase input voltage to intermediate high 400V DC voltage bus by use of 6 or more controllable switches. The second Isolated DC/DC converter stage then provides isolation and conversion to lower DC voltages, such as 48V or 12V. Unfortunately, all present isolated DC/DC converters must store the DC output energy in the form of output filtering inductor carrying DC load current.

The problem lies in the premature rectification of the AC line into an intermediate 400V DC voltage. The instantaneous power delivered to DC load is constant. Therefore, there is no conceptual reason, why the constant instantaneous three-phase input power could not be converted directly into a constant DC output power. The obvious added advantage is that such AC/DC conversion will completely eliminate need for energy storage. Furthermore, the power conversion will take place in a single power processing stage as seen in the new Three-Phase Rectifier illustrated in Figure 12 which consists of three Isolated Bridgeless PFC converters, one for each phase, of the type shown in Figure 8.

Additional important efficiency and size advantages are obtained as well. For example, the total power is delivered through three parallel paths so that each phase processes only one third of total output power. The overall efficiency stays the same at 98% as the efficiency of isolated converters in each phase. Similarly the same low THD distortion and high power factor of 0.999 of each phase is also preserved.

Finally, the instantaneous output currents of each phase are positive and fluctuating in time in sinusoidal manner. However, due to 120-degree displacement of the input line currents of each phase, all fluctuating output currents of each phase add up to constant output current as illustrated in Figure 1. Any remaining ripple current is on the order of 5% of the DC load current and comes at the filtering frequency, which is six times higher than the fundamental 60Hz frequency. This clearly results in much reduced size of filtering capacitors needed, hence in reduced size and cost of the three-phase rectifier.

Alternative isolated bridgeless PFC converter topologies

The converter topology of Figure 8 is not the only True Bridgeless PFC converter topology with isolation. Another Single-stage AC/DC converter topology with PFC and isolation is shown in Figure 13 which can be used either as a Single-phase Rectifier or implemented in converter of Figure 12 as a Three-Phase Rectifier. This converter has the same DC voltage gain of the boost type such as [1] and has only one magnetic piece, the two winding isolation transformer, which does have a DC bias and is therefore

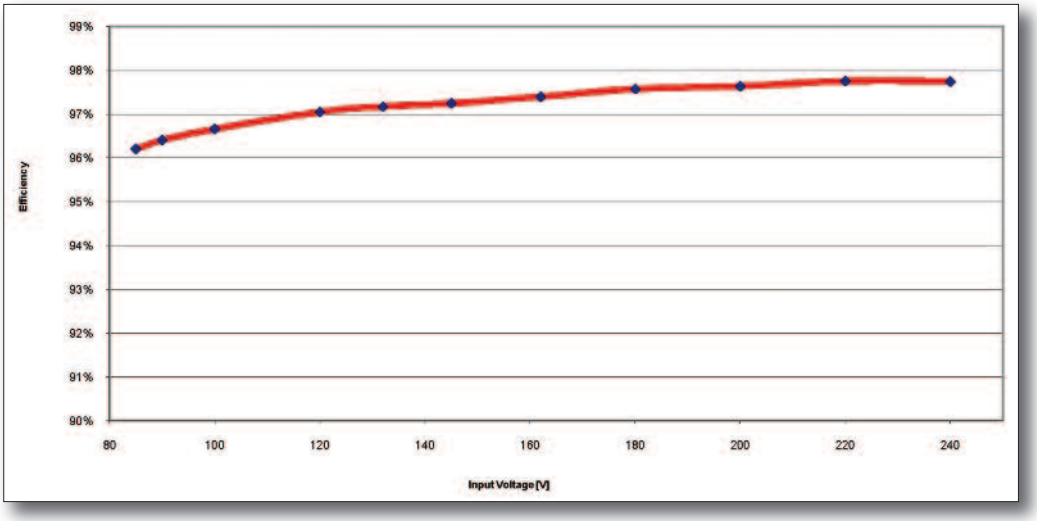

Figure 11: Efficiency measurements show near 98% efficiency at high line of 240V AC

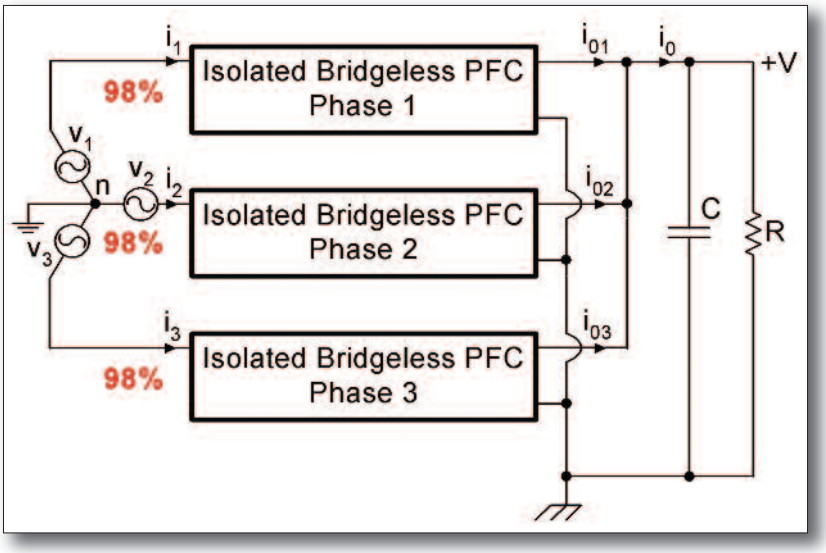

Figure 12: Three-Phase Rectifier consisting of three Isolated Bridgeless PFC converters, one for each phase, of the type shown in Figure 9

suitable for low to medium power. In addition, the input current is pulsating requiring the use of the separate high frequency filter on input to reduce ripple currents at high switching frequency.

The applications above have highlighted the use of the new boost converter topologies, the inverting and non-inverting ones, for a single-stage True Bridgeless AC/DC power conversion and their application for single- and three-phase rectifiers which include galvanic isolation at high switching frequency. However, the new boost converter topologies have also significant advantages when applied to isolated DC/DC conversion.

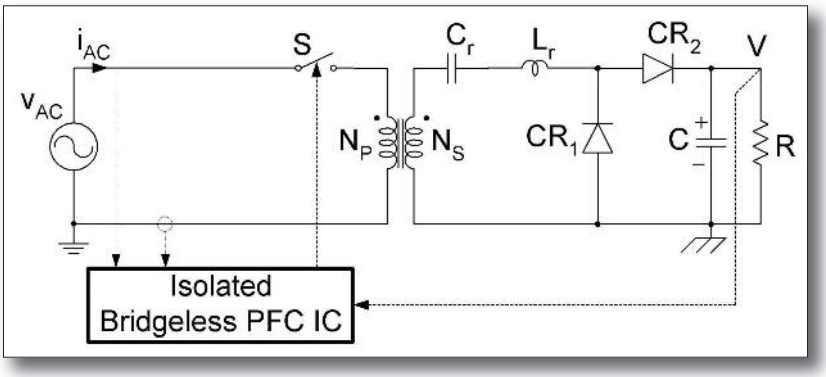

Figure 13: True Bridgeless isolated PFC Converter featuring two winding isolation transformer

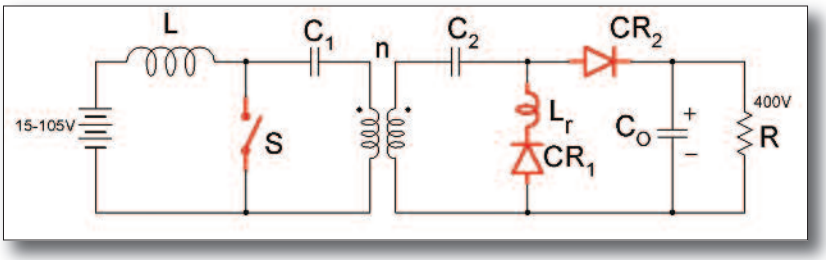

Figure 14: Isolated Boost DC/DC converter for converting solar cell input power into a high voltage 400V DC bus

Shown in Figure 14 is the new isolated boost DC/DC converter [4] used for converting solar cell input power into a high voltage 400V DC bus. It can accommodate the wide range of the input voltage of 15V to 100V (created by the variation of solar cells voltages during the day) and generate regulated high DC voltage isolated output of 400V with efficiencies of over 97%.

In current automotive applications for hybrid and electric vehicles, the auxiliary 1kW to 2kW converters are needed to convert the 400V battery voltage of the high voltage DC bus to 14V auxiliary battery voltage and vice versa. Therefore a bi-directional buck-boost converter is needed. The converter of Figure 14 implemented with MOSFET switches instead of current rectifiers on the output is capable of such bi-directional power flow in a single power processing stage and is well suited for these applications. Once again, the use of three switches only instead of eight switches of conventional converters results in increased efficiencies and reduced cost at the same time.

Literature

[1] Slobodan Ćuk, "Modeling, Analysis and Design of Switching Converters", PhD thesis, November 1976, California Institute of Technology, Pasadena, California, USA.

[2] Slobodan uk, R.D. Middlebrook, "Advances in Switched-Mode Power Conversion, " Vol. 1, II, and III, TESLAco 1981 and 1983.

[3] Slobodan Ćuk, articles in Power Electronics Technology, describing Single-Stage, Bridgeless, Isolated PFC Converters published in July, August, October and November 2010 issues.

[4] Slobodan Ćuk and Zhe Zhang, Voltage Step-up Switching DC-DC Converter, US patent No. 7,778,046, August 17, 2010.

[5] 99% Efficient AC/DC Converter Topologies, Power Electronics Europe 3/2011

[6] Slobodan Ćuk, "Single-Stage, AC-DC Converter Topologies of 98% Efficient Single Phase and Three-Phase Rectifiers", Keynote at PCIM Europe 2011, May 17, Nuremberg, Germany